Mathematical Modeling of Continuously Variable Transmission (CVT) System

Sarah Crosby*
Department of Engineering Mathematics
Faculty of Engineering, Alexandria University
Alexandria, Egypt

Galal Elkobrosy
Department of Engineering Mathematics
Faculty of Engineering, Alexandria University
Alexandria, Egypt

Hassan Elgamal
Department of Mechanical Engineering
Faculty of Engineering, Alexandria University
Alexandria, Egypt

Abstract—**A continuously variable transmission (CVT) provides an infinite number of gear ratios between two finite limits. This allows the engine to run at its most efficient RPM independent of the car speed, making CVT the most efficient transmission system. The CVT is also fuel efficient, because it reduces the engine speed at high vehicle speed and allows the engine to run at its optimal point.**

Aiming at determining the behavior of the CVT transmission, a complete mathematical model have been constructed for the whole vehicle equipped with CVT, simulating the whole vehicle dynamics. The model takes into consideration each component of the vehicle, including: the engine dry friction disc clutch, belt type CVT, car differential, wheels and body. In this paper, the slip between the belt and the pulleys and the CVT traction curve were considered. The kinematical, geometrical and momentum equations governing the performance of the whole system were formulated and solved. The governing differential equations were numerically solved In order to predict the behavior of the different mechanical parts of the system. The results of the simulation shows that the system becomes steady after a short period of time. The analysis of the system's dynamical response demonstrates that the simulation model established represents the system efficiently.

Keywords— Automatic Transmission; Continuously variable transmission; Mathematical Modeling; Transmission; ; V-belt CVT

I. INTRODUCTION

Over the last decades, a growing attention has been focused on the environmental question. Governments are continuously forced to set standards and to adopt actions in order to reduce the polluting emissions and the green-house gasses. In order to fulfil these requirements, car manufacturers have been obligated to dramatically reduce vehicles' gas emissions. The continuously variable transmission (CVT) represents one of the most promising solution, which is able to provide an infinite number of gear ratios between two finite limits. The CVT optimizes the engine working conditions, gets the highest efficiency, and therefore, improves fuel saving and reduces greenhouse gases emissions

With the lack of oil and the call for reducing the environmental pollutants, the number of cars equipped with CVT has significantly increased. Up to now, more than one billon cars have been equipped with continuously variable transmission all over the world. Especially the metal belt type continuously variable transmission is applied widely. CVT has wide change range of speed ratio and it can adjust the ratio continuously and automatically according to the situation of running to maintain the engine to work in economy mode or power mode all the time. For this reason, CVT equipped cars are more economical than cars equipped with planetary gear automatic transmissions. The key advantages of a CVT that interest vehicle manufacturers and customers can be summarized as: higher engine efficiency, higher fuel economy, smooth acceleration without shift shocks and Infinite gear ratios with a small number of parts.

A continuously variable transmission (CVT) is an automatic transmission that can change seamlessly through an infinite number of effective gear ratios between maximum and minimum values by changing the diameters of input shaft and output shaft directly, instead of going through several gears to perform gear ratio change. This contrasts with other mechanical transmissions that offer a fixed number of gear ratios. The most common type of CVT used is the pulley based CVT. The variable-diameter pulleys are main component of the pulley-based CVT. Each pulley is made of two 20-degree cones facing each other. A belt rides in the groove between them, as shown in Fig.1.

Variable-diameter pulleys must always come in pairs, as shown in Fig.2, one of the pulleys, known as the driving pulley, is connected to the crankshaft of the engine, and the second pulley is called the driven pulley. When one pulley increases its radius, the other decreases its radius to keep the belt tight. As the two pulleys change their radii relative to one another, they create an infinite number of gear ratios.

Aiming to achieve an optimal CVT performance and a significant reduction of fuel consumption, it is fundamental to have a very good control strategy of the transmission, which in turns needs a reliable model of the CVT mechanical behavior.
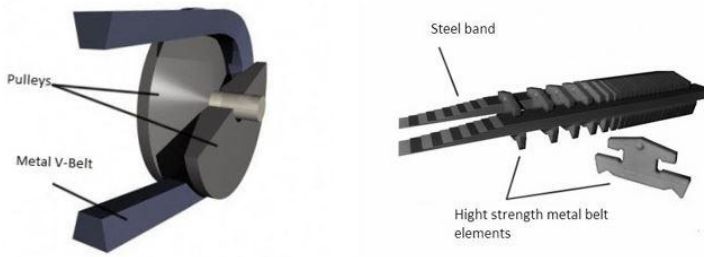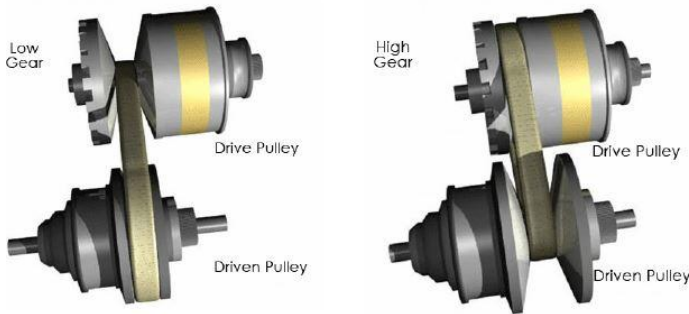
Fig.1 Layout of CVT V-belt

Fig.2 Pulley based CVT structure

Gerbert [1, 2] worked on understanding the mechanics of traction belts, especially metal pushing V-belts and rubber V-belts. He used quasi-static equilibrium analysis to develop a set of equations that capture the dynamic interactions between the belt and the pulley. Since the belt is capable of moving both radially and tangentially, variable sliding angle approach was implemented to describe friction between the belt and the pulley. Gerbert [3] also analyzed the slip behavior of a rubber belt CVT. He also discussed slip during wedging due to poor fit between the belt and the pulley.

Kim and co-workers [4,5] investigated the metal belt behavior analytically and experimentally. They proposed a speed ratio–torque load–axial force relationship to calculate belt slip. They obtained the equations of motion using quasi-static equilibrium conditions and reported that the gross slip points depend on the torque transmitting capacity of the driven side. Bonsen et al. [6] analyzed slip and efficiency in a metal pushing V-belt CVT. They stated that high clamping force reduces the efficiency of a CVT. However, high clamping forces are necessary to avoid excess slip between the belt and the pulley.

Sferra et al. [7] developed a unique model of a metal V-belt CVT in order to simulate its transient behavior. The model included inertial and pulley deformation effects. Discrete and continuous shifting behaviors were simulated in order to analyze efficiency and power losses due to friction between the belt and the pulley halves. The results showed high loss of efficiency during shifting transients.

Bullinger and Pfeiffer [8,9] developed a detailed elastic model of metal V-belt CVT system to determine its power transmission characteristics at steady state. Pulley, shaft, and belt deformations were taken into account. The frictional constraints were modeled using the theory of unilateral constraints.

Sattler [10] analyzed the mechanics of a metal chain and V-belt considering longitudinal and transverse stiffness of the chain/belt, and pulley misalignment and deformations. The pulley was assumed to deform in two ways, pure axial deformation and a skew deformation. The model was primarily used to study efficiency aspects of belt and chain CVTs.

Carbone et al. [11] proposed a model that describes both the steady-state and the shifting dynamics of the V-belt CVT. The belt was modeled as a one-dimensional continuous body with zero radial thickness and infinite axial stiffness. Later, Carbone et al. [12] investigated the influence of pulley deformation on the shifting mechanism of a metal V-belt CVT. Coulomb friction hypothesis was used to model friction between different surfaces. Flexural effects of the belt were neglected; however, pulley bending was considered based on Sattler's model [10].

Although there are many researches modeling and describing the dynamics of the CVT, the majority of these researches aimed only at modeling the CVT variator without modeling the complete vehicle system.

In this paper, a complete model for the whole vehicle equipped with CVT, including all the vehicle components; car engine, friction disc clutch, CVT, car differential, wheels and car body has been constructed.

This paper puts forward the mathematical model of CVT system including pulley the slip between the pulley and the CVT belt. The kinematical, geometrical and momentum equations governing the performance of the CVT system were formulated and solved. The numerical solution of these equations predicts the behavior of the different mechanical parts of the system.

II. MATHEMATICAL MODEL

The whole vehicle is modeled including the engine, the clutch, the CVT, the car differential and the wheels. As shown in Fig. 3, the model is composed of engine, dry friction disc clutch, belt type CVT, car differential, wheels and body.

The following dimensionless conversions will be used throughout the mathematical model:

Dimensionless radius: $R^* = \frac{R}{c}$

Dimensionless time: $t^* = t\ \Omega$

Dimensionless angular speed: $\omega^* = \frac{\omega}{\Omega}$

Dimensionless force: $F^* = \frac{F}{\Omega^2 c^2 \sigma}$

Dimensionless torque: $T^* = \frac{T}{\Omega^2 c^3 \sigma}$

Dimensionless moment of inertia: $J^* = \frac{J}{c^3 \sigma}$

Where, Ω is the reference angular speed, c is the center distance between the two pulleys and σ is the belt mass density.

A. The Engine Model

Engine model is developed by applying Newton's second law to the rotational dynamics of the engine:

$$J_e \omega_e^{\cdot} + B_e \omega_e = T_e - T_{cl} \tag{1}$$

Fig. 3 Simplified model of transmission system

Where T_e is the engine torque, J_e is the rotary inertia of the engine , and ω_e is the acceleration of the engine. The engine torque T_e is assumed to be a function of the engine's rotational speed ω_e and the throttle angle opening φ. The relationship between T_e and ω_e is deduced from the engine's performance map shown in Fig. 4, where there is a separate curve for each position of the accelerator.

$$T_e = T_{map}(\omega_e, \varphi) \qquad (2)$$

Tabulated torques values are used to represent the relationship between engine torque, throttle opening and engine speed. These values are entered into Matlab curve fitting tool based on the engine performance map, as depicted in Fig. 5. The torque values are obtained by polynomial curve fitting in Matlab to get torque at any speed and throttle position.

Fig.4 Engine Performance Map [14]

These torque values are used in Eq. (1) to get engine acceleration which is then integrated to obtain engine speed.

To obtain the non-dimensional engine torque Te^*:

$$Te^* = \frac{T_{e_{map}}}{\sigma \, \Omega^2 \, c^8} \qquad (3)$$

Fig.5 Curve Fitting of the Engine Performance Map

B. The Clutch Model

A dry friction clutch type is used in the model [13]. It consists of a housing, pressure plates, friction plates, a clutch disc with torsion "dampers" and a release mechanism. The clutch is normally closed as the diaphragm spring is pre-tensioned when assembled .The clutch disc is equipped with torsional dampers which are coil springs that connect various segments of the clutch disc. These coil springs aim at maximizing the comfort level for the driver, when opening and closing the clutch

The clutch system is modelled as shown in Fig. 6. The clutch disc has inertia J_{cl}. The torque transmitted through the clutch is T_{cl}. The angular speed of the clutch disc is presented by ω_{cl}.

Fig. 6 Powertrain model

The angular displacement of the damper springs is ϕ_d. Where $\phi_d = \phi_{cl} - \phi_t$, where ϕ_{cl} is the clutch angular displacement and ϕ_t is the transmission angular displacement. The nonlinear stiffness of the damper coil springs $k(\phi_d)$ is simplified into the form [13]:

$$k(\varphi_d) = \begin{cases} 60 & \left(\frac{N.\,m}{rad}\right) & for - 0.25 \leq \emptyset_d \leq 0.35, \\ 1000 & \left(\frac{N.\,m}{rad}\right) & else \end{cases} \qquad (4)$$

The differential equations governing the clutch dynamics can be expressed as:

$$J_{cl}\,\omega_{cl}' + B_{cl}\,\omega_{cl} = T_{cl} - T_p \qquad (5)$$

$$T_p' = k(\phi_d).(\omega_{cl} - \omega_p) \qquad (6)$$

The torque through the clutch while slipping is given by:

$$T_{cl} = F_n.\,\mu_{cl}.\,R_d\,.sign(\omega_e - \omega_{cl}) \qquad (7)$$

In which μ_{cl} is the friction coefficient of the clutch surface material, R_d is the active radius of the clutch plates and the normal actuation force on the clutch plate is given by F_n.

The dimensionless clutch torque can be obtained by:

$$T_{cl}^* = \frac{F_n^* \cdot \mu_{cl} \cdot R_d}{c}\,.sign(\omega_e^* - \omega_{cl}^*) \qquad (8)$$

Where:

$$F_n^* = \frac{F_n}{\Omega^2\,\sigma\,c^2} \qquad (9)$$

C. CVT and drive shafts:

1) CVT Model Assumptions

The model that will be presented is derived by making the following assumptions and simplifications:

a) The metal belt is considered as a one-dimensional continuous body, with locally rigid motion. This means there is no longitudinal and transversal deformation, i.e. the belt is considered to be an inextensible strip with zero radial thickness and infinite axial stiffness.

b) The bending stiffness of the belt is neglected.

c) The Coulomb friction coefficient µ, acting between the segments and the pulleys, has a constant value.

2) CVT system Mechanics

In Fig.7 the entire CVT system is shown, where the driving, the driven pulley and the belt are presented. The moving half pulleys are subject to active axial forces which can be changed to obtain a variation of the belt's pitch radii and thus modify the speed ratio.
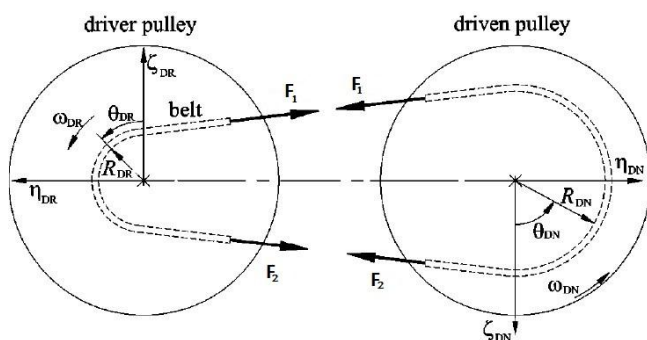
Fig.7 CVT Scheme

In Fig.8, the kinematical and geometrical quantities involved are shown, and the plane $\pi_{r\theta}=[e_r,e_\theta]$ is illustrated. The figure shows the sliding angle γ, the angular coordinate θ, the radial coordinate r, the radius of curvature ρ and the slope angle φ. Moreover, the tangent unit vector τ of the belt and the corresponding normal unit vector n are represented in addition to the radial and circumferential unit vectors e_r and e_Θ.

3) Geometric and Kinematic Equations

By observing Fig.8, the following relations can be derived:

$$\tan(\varphi) = \frac{1}{r}\cdot\frac{\partial r}{\partial \theta} \qquad (10)$$

$$\delta l = \frac{r}{\cos(\phi)}\,\delta\theta \qquad (11)$$

$$\frac{1}{\rho} = \frac{\cos(\varphi)}{r}\cdot\left(1 - \frac{\partial\varphi}{\partial\theta}\right) \qquad (12)$$

$$r.\omega_d = \dot{r}.\tan(\gamma) \qquad (13)$$

$$\tan(\beta_s) = \tan(\beta)\;\cos(\gamma) \qquad (14)$$

Where ω_d is the local sliding angular velocity of the belt, and δl, δθ are the length and the angular extension of a material element of the belt respectively. Equation (13) correlates the radial velocity of the belt with its sliding tangential velocity, while (14) relates the half-opening angle βs in the sliding plane with the sliding angle γ.
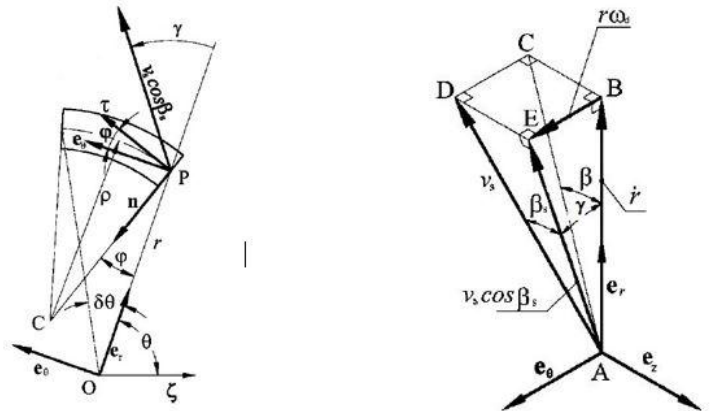

Fig.8 Kinematical and Geometric Quantities

4) Continuity Equation

According to [11], the continuity equation can be written as:

$$\frac{r}{r} + \frac{\partial\omega_s}{\partial\theta} = 0 \qquad (15)$$

This equation is based on the assumption that the belt is inextensible, that the longitudinal and transverse deformations are neglected and that the elongation of the belt is also neglected.

5) Momentum Equations

The forces involved in the equilibrium of the belt involves the tension of the belt (F), the linear pressure acting on the belt sides (P), the friction force (f_a), and the inertia force of the belt element due to its acceleration ($\sigma\,\omega^2 R^2\,d\theta$).This is visualized in Fig.9. The friction force $f_a =\mu$. p. And the net tension of the belt; F=T-P.

Where T is the tension of the band and P is the compressive forces between metal segments

According to [11], the following assumptions are made to calculate the equilibrium:

a) It is possible to calculate the local angular acceleration θ of the considered belt's material element with the pulley's angular velocity ω.

b) From Eq. (12), it follows that $\rho \approx r \approx R$, therefore all these three parameters are written as R.

c) The term $\ddot{R}$ is neglected with respect to $\omega^2 R$, i.e. $\left| \frac{\ddot{R}}{\omega^2 R} \right| \ll 1$

d) $\phi \ll 1$.

e) The belt's axial and tangential acceleration are neglected.

With these assumptions, the two Momentum Equations are:

$$\frac{1}{F - \sigma . \omega^2 . R^2} \frac{\partial (F - \sigma . \omega^2 . R^2)}{\partial \theta} = \frac{\mu . \cos\beta_s . \sin(\gamma)}{\sin\beta - \mu . \cos\beta_s . \cos\gamma} \quad (16)$$

$$p = \frac{F - \sigma . \omega^2 . R^2}{2R (\sin\beta - \cos\beta_s . \cos\gamma)} \quad (17)$$
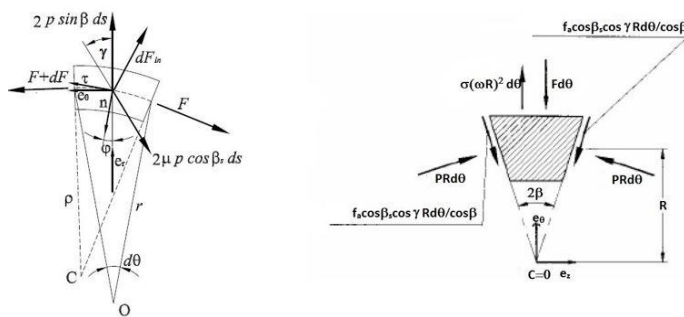
Fig.9 Forces acting on belt

6) Dimensionless Equations

A new angular coordinate $\hat{\theta}$ is defined as the angular coordinate of the real or imaginary point at which the sliding velocity's component of the belt in $\pi_{r\theta} = [e_r , e_\theta]$ plane is purely radially directed. Equations (10) and (15) can be reformulated as:

$$\phi = \frac{1}{r} \partial r / \partial \theta \quad (18)$$

$$V_r + \frac{\partial v_\theta}{\partial \theta} = 0 \quad (19)$$

Where V_r is the radial sliding velocity of the belt = $r \cdot$, and V_θ is the tangential sliding velocity of the belt = $r \ \omega_d$ .All the previously derived relations can be rephrased in dimensionless form once the following dimensionless quantities can be defined:

Dimensionless radial velocity: $w = \frac{R}{\omega R}$ (20)

Local sliding coefficient:
$s_c = \omega_d / \omega$ (21)

Dimensionless belt's tension: $K = \frac{F - \sigma R^2 \omega^2}{\hat{F} - \sigma R^2 \omega^2}$ (22)

Dimensionless linear pressure: $\tilde{p} = \frac{p . R}{\hat{F} - \sigma R^2 \omega^2}$ (23)

Dimensionless belt radial velocity: $\tilde{v}_r = \frac{r}{\omega r} \frac{1}{\Delta} \frac{\sin(2\beta)}{1 + \cos^2 \beta}$ (24)

Dimensionless belt tangential velocity: $\widetilde{v_\theta} = \frac{\omega_s}{\omega} \frac{1}{\Delta} \frac{\sin(2\beta)}{1 + \cos^2 \beta}$ (25)

Rewriting the previously derived relations in terms of the new dimensionless terms to get simpler form; (13) can be written into:

$$\tan\gamma = \frac{\tilde{v}_r}{\tilde{v}_\theta} \quad (26)$$

Equations (16) and (17) can be rephrased as follows:

First Momentum Equation:

$$\frac{\partial k}{k \partial_\psi} = \frac{\mu \cos\beta_s \sin\gamma}{\sin\beta - \mu \cos\beta_s \cos\gamma} \quad (27)$$

Second Momentum Equation:

$$\tilde{p} = \frac{k}{2(\sin\beta - \mu \cos\beta_s \cos\gamma)} \quad (28)$$

Continuity Equation:

$$\frac{\partial s_c}{\partial_\psi} + w = 0 \quad (29)$$

Kinematic Equation:

$$s_c = w . \tan\gamma$$
(30)

Geometric Equation:
$$\tan(\beta_s) = \tan(\beta) . \cos(\gamma) \quad (31)$$

7) Graphical Representation of λ, δ and ξ

λ is defined as the traction coefficient and the force ratio is defined as:

$$\xi = \frac{k2}{k1} = \frac{F_2 - \sigma R^2 \omega^2}{F_1 - \sigma R^2 \omega^2} \quad (32)$$

The values of λ and ξ [11] are entered into Matlab curve fitting tool, in order to illustrate the relation between λ and ξ , for w<0 and w>0, as shown in Fig.10. The values of the ratio δ= S / $[(F_1 - \sigma R^2 \omega^2) + F_2 - \sigma R^2 \omega^2)] = \tilde{S} / (k_1 + k_2)$ versus the force ratio ξ [11], were obtained by polynomial curve fitting in Matlab to represent the relationship between δ and ξ, as shown in Fig.11.
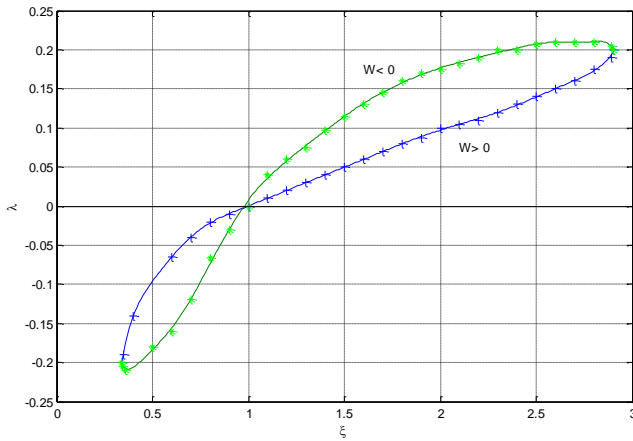
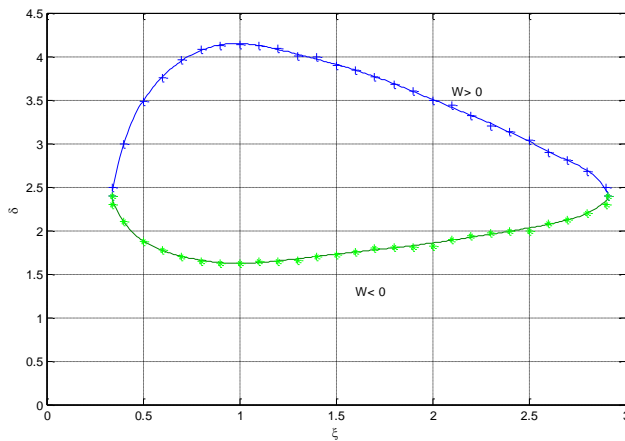Fig.10 Traction coefficient λ versus force ratio ξ (μ=0.1, β=18°)

Fig.11 Dimensionless Ratio δ versus force ratio ξ (μ=0.1, β=18°)

8)   *Slip in a Continuously Variable Transmission*

The clamping force should be large enough to prevent the slip between the belt and the pulleys. On the other hand, a large clamping force reduces the efficiency of the Continuously Variable Transmission (CVT). Hence, it is important to estimate and control the right amount of slip.

The traction curve shown in Fig.12 [6], gives the relation between the transmitted torque and the slip. The traction coefficient λ is defined as [16]:

$$\lambda_p = \frac{T_p \cos\beta}{2 F_p R_p} \qquad , \qquad \lambda_s = \frac{T_s \cos\beta}{2 F_s R_s} \tag{33}$$

In which T_p is the primary pulley torque, T_s is the secondary pulley torque, R_s is the secondary running radius of the belt on the pulley, R_p is the primary running radius of the belt on the pulley, F_s is the secondary clamping force, and F_p is the primary clamping force. λ_p and λ_s are assumed to have the same value, i.e. ($\lambda_p = \lambda_s = \lambda$).The second variable in the traction curve is the slip in the variator; slip is defined as:

$$s = \left| 1 - \frac{\omega_s}{\omega_p \, . n} \right| \tag{34}$$

Where, ω_s is the angular speed of the secondary axle, ω_p is the angular speed of the primary axle and n is the geometrical ratio, which is defined by:

$$n = \frac{R_p}{R_s} \tag{35}$$

Using the experimental data of [6], the traction coefficient λ is obtained as a function of the percentage slip s, for different drive ratios.
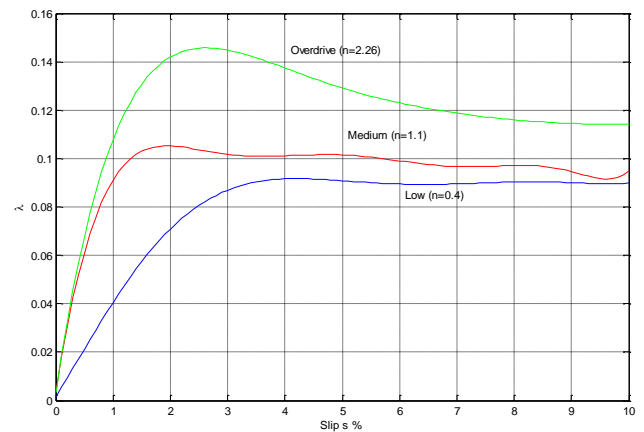

Fig. 12 Traction coefficient λ as a function of slip measured at 300rad/s, for ratios low (0.4), Medium (1.1) and overdrive (2.26) [6]

9)   *Derivation of the equation of the angular speed of the CVT primary and secondary pulley*

From Fig.3 we can obtain the dynamic equation of the angular speed of the CVT secondary pulley as follows:

$$J_s \, \dot{\omega}_s + B_s \, \omega_s = T_s - T_o \tag{36}$$

To obtain the governing equation of the primary pulley angular speed:

First, by differentiating the slip equation (34), we have:

$$\frac{ds}{dt} = -\left[\frac{\omega_s}{\omega_p \, n} - \frac{\omega_p \, \omega_s}{\omega_p^2 \, n} - \frac{n \, \omega_s}{n^2 \, \omega_p} \right] \tag{37}$$

Then, by substituting $\dot{\omega}_s$ from (36) and substituting $\frac{\omega_s}{\omega_p \, n}$ from the slip equation (34); (37) becomes:

$$\frac{ds}{dt} = -\frac{1}{\omega_p} \left[\frac{(T_s - T_o)}{J_s \, n} - \frac{B_s \, \omega_s}{J_s \, n} - \dot{\omega}_p \, (1-s) - \frac{n \, \omega_s}{n^2} \right] \tag{38}$$

Therefore,

$$\dot{\omega}_p = \frac{1}{1-s} \left[\frac{(T_s - T_o)}{J_s \, n} - \frac{B_s \, \omega_s}{J_s \, n} - \frac{\omega_s \, \dot{n}}{n^2} + \omega_p \, \frac{ds}{dt} \right] \tag{39}$$

And in dimensionless form:

$$\frac{d\omega_p^{\ast}}{dt^{\ast}} = \frac{1}{1-s}\left[\frac{(T_s^{\ast}-T_o^{\ast})}{n} - \left(\frac{B_s}{J_s\,\Omega}\right)\omega_s^{\ast} - \left(\frac{1}{n^2}\frac{dn}{dt^{\ast}}\right)\omega_s^{\ast} + \omega_p^{\ast}\cdot\frac{ds}{dt^{\ast}}\right] \quad (40)$$

In order to obtain $\frac{ds}{dt^{\ast}}$:

By differentiation the traction coefficient equation (33) w.r.t time we get:

$$T_p^{\ast} = \frac{2\,F_p\,R_p\,\lambda_p}{cos\beta} \quad (41)$$

From the clutch model equation, (6) and from (41), we have:

$$\frac{2\,F_p\,R_p\,\lambda_p}{cos\beta} = k(\phi).(\omega_{cl} - \omega_p) \quad (42)$$

But, $\frac{d\lambda_p}{dt} = \frac{d\lambda_p}{ds} \ast \frac{ds}{dt}$. Let $\Gamma = \frac{d\lambda_p}{ds}$

Therefore,

$$\frac{d\lambda_p}{dt} = \Gamma \ast \frac{ds}{dt} \quad (43)$$

From the traction coefficient equation (33):

$$\frac{2\,F_p\,R_p}{cos\beta} = \frac{T_p}{\lambda_p} \quad (44)$$

Substituting from (44) into (42) we get,

$$\frac{T_p}{\lambda_p}\frac{d\lambda_p}{dt} = k(\phi).(\omega_{cl} - \omega_p) \quad (45)$$

Substituting from (45) into (34) we get,

$$\frac{ds}{dt} = \frac{1}{\Gamma}\frac{\lambda_p}{T_p}\frac{d\lambda_p}{dt}k(\phi).(\omega_{cl} - \omega_p) \quad (46)$$

In dimensionless form:

$$\frac{ds}{dt^{\ast}} = \frac{\lambda_p}{\Gamma}\frac{1}{T_p^{\ast}}\left[\frac{k(\phi)}{\sigma\,\Omega^2 c^3}\right](\omega_{cl}^{\ast} - \omega_p^{\ast}) \quad (47)$$

10) Calculation of dimensionless primary and secondary radius

The values of the radii of the primary and secondary pulleys are functions of the ratio between the belt length and the center distance of the two pulleys. The length of the belt can be calculated from the following relation:

$$L = \pi(R_p + R_s) + 2(R_s - R_p)sin^{-1}\left(\frac{R_s - R_p}{C}\right) + 2\sqrt{C^2 - (R_s - R_p)^2} \quad (48)$$

Dividing the previous equation by the center distance, we have:

$$\frac{L}{C} = \left(\frac{\pi R_p}{C}\right)\left(\frac{1+n}{n}\right) + \left(\frac{2R_p}{C}\right)\left(\frac{1-n}{n}\right)sin^{-1}\left[\frac{R_p(1-n)}{Cn}\right] + 2\sqrt{1 - \frac{R_p^2}{C^2}\left(\frac{1-n}{n}\right)^2} \quad (49)$$

The belt length in dimensionless form is given by:

$$L^{\ast} = \pi R_s^{\ast}(1+n) + 2R_s^{\ast}(1-n)sin^{-1}[R_s^{\ast}(1-n)] + 2\sqrt{1 - R_s^{\ast 2}(1-n)^2} \quad (50)$$

Assuming the value of $L^{\ast}$ and getting the roots of the non-linear equation of y using Matlab, the values of $R_p^{\ast}$ and $R_s^{\ast}$ can be calculated.

11) Evaluation of the values of δ, λ and ξ

The non-dimensional ratio λ is obtained by using the λ versus slip relation, in Fig.12, knowing the value of speed ratio 'n' and the allowed value of slip percentage. And ξ is obtained from the relation between λ and ξ in Fig.10, according to the sign of dimensionless radial velocity W_s.

Where:

$$W_s = \frac{R_s}{R_s\omega_s} = \frac{-\dot{n}}{\omega_s\cdot\left\{\frac{\pi+2sin^{-1}[R_s^{\ast}(1-n)]}{\pi-2sin^{-1}[R_s^{\ast}(1-n)]}\right\}+n} \quad (51)$$

The ratio δ is obtained from the relation between δ and ξ in Fig.11, according to the sign of the dimensionless radial velocity W_s.

12) Evaluation of the primary and secondary torques
Since,

$$\delta_s = \frac{F_s^{\ast}}{F_{t_1}^{\ast} + F_{t_2}^{\ast} - 2R_s^{\ast 2}\omega_s^{\ast 2}}$$

Hence,

$$F_{t_1}^{\ast} + F_{t_2}^{\ast} = 2R_s^{\ast 2}\omega_s^{\ast 2} + \frac{F_s^{\ast}}{\delta_s} \quad (52)$$

Since,

$$\xi_s = \frac{(F_{t_2}^{\ast} - R_s^{\ast 2}\omega_s^{\ast 2})}{(F_{t_1}^{\ast} - R_s^{\ast 2}\omega_s^{\ast 2})}$$

Hence,

$$F_{t_1}^{\ast}\xi_s - F_{t_2}^{\ast} = R_s^{\ast 2}\omega_s^{\ast 2}(\xi_s - 1) \quad (53)$$

From (33) we have,

$$F_s^{\ast} = \frac{(F_{t_1}^{\ast} - F_{t_2}^{\ast})cos\beta}{2\lambda_s} \quad (54)$$

Substituting from (54) into (52):

$$F_{t_1}^{\ast}(2\lambda_s\delta_s - cos\beta) + F_{t_2}^{\ast}(2\lambda_s\delta_s + cos\beta) = 4R_s^{\ast 2}\omega_s^{\ast 2}\lambda_s\delta_s \quad (55)$$

Substituting From (53) into (55)

$$F_{t_1}{}^{\bullet}(2\,\lambda_s\delta_s - cos\beta) + (2\,\lambda_s\delta_s + cos\beta)(F_{t_1}{}^{\bullet}\,\xi_s - R_s{}^{\bullet 2}\omega_s{}^{\bullet 2}\,(\xi_s - 1) = 4\,R_s{}^{\bullet 2}\omega_s{}^{\bullet 2}\lambda_s\delta_s \tag{56}$$

From (56):

$$F_{t_1}{}^{\bullet} = \frac{\omega_s{}^{\bullet 2}R_s{}^{\bullet 2}\,[\xi_s\,(2\,\lambda_s\,\delta_s + cos\,\beta_o) - cos\,\beta_o + 2\,\lambda_s\,\delta_s]}{(2\,\lambda_s\delta_s - cos\,\beta_o) + \xi_s\,(2\,\lambda_s\delta_s + cos\,\beta_o)} \tag{57}$$

From Eq. (56) into Eq. (53)

$$F_{t_2}{}^{\bullet} = R_s{}^{\bullet 2}\omega_s{}^{\bullet 2}\left\{\frac{[\xi_s\,(2\,\lambda_s\,\delta_s + cos\,\beta_o) - cos\,\beta_o + 2\,\lambda_s\,\delta_s]\,.\xi_s}{(2\,\lambda_s\delta_s - cos\,\beta_o) + \xi_s\,(2\,\lambda_s\delta_s + cos\,\beta_o)} - (\xi_s - 1)\right\} \tag{58}$$

Hence,

$$F_{t_2}{}^{\bullet} = \frac{[(2\,\lambda_s\,\delta_s - cos\,\beta_o) + \xi_s\,(2\,\lambda_s\,\delta_s + cos\,\beta_o)]\,\omega_s{}^{\bullet 2}R_s{}^{\bullet 2}}{(2\,\lambda_s\,\delta_s - cos\,\beta_o) + \xi_s\,(2\,\lambda_s\,\delta_s + cos\,\beta_o)} \tag{59}$$

$$T_p{}^{\bullet} = (F_{t_1}{}^{\bullet} - F_{t_2}{}^{\bullet})\,R_p^{\bullet} \tag{60}$$

And,

$$T_s{}^{\bullet} = (F_{t_1}{}^{\bullet} - F_{t_2}{}^{\bullet})\,R_s^{\bullet} \tag{61}$$

D. Car Differential, wheels and Resistive Load

The car differential splits the engine torque on the left and right transmission branches while allowing for different revolution speeds on the two shafts. The two powered wheels (usually the front wheels) are described with a single inertia J_w. A resistance load Torque is acting on the vehicle and impeding its motion. This resistive torque consists of aerodynamic drag resistance, rolling resistance, gradient resistance and inertia resistance.

1) Aerodynamic Drag Resistance
The force due to aerodynamic drag depends mainly on the shape of the vehicle, the density of the surrounding air, and the velocity of the vehicle. The equation for the aerodynamic drag force is:

$$\text{Drag Force} = \frac{1}{2}\,C_D\,A\,\rho_{air}\,u^2 \tag{62}$$

Where:
C_D = Coefficient of aerodynamics resistance (drag coefficient)
A= Car frontal area [m^2]
ρ_{air} = Air density [kg/m^3]
u = Car velocity [m/s]

2) Rolling resistance
Rolling resistance= G. f. $cos\,\theta_r$ (63)

Where:
f = coefficient of rolling resistance
G= car weight [N]
m = car mass [kg]
g = Acceleration due to gravity
θ_r =the angle of road inclination

3) Gradient resistance
The gradient resistance depends on the angle of the road inclination and the weight of the car. The gradient resistance is given by:
Gradient resistance= ± G sin θ_r (64)

Where:
$\pm$
$$\begin{cases} (+)\text{with the car going up hill (ascending)(resistance effort)} \\ (-)\text{With the car going down hill (descending) (tractive effort)} \end{cases}$$

4) Inertia Resistance
When the car changes its velocity (accelerate or decelerate), it needs a force, this force is represented by the car resistance to change its speed (inertia force). This force depends on the mass of the car and the value of the car acceleration.

Inertia Resistance= ± (m+m$_{eq}$). a (65)

Where:
a = car acceleration [m/s^2]
m_{eq} =equivalent mass of rotating parts [kg]

$$m_{eq} = \frac{J_r}{r_w{}^2} + \frac{J_w}{r_w{}^2}\,.\,n_o{}^2.n^2.\eta$$

Where:
J_w= The equivalent rotary inertia of wheels
J_r = The equivalent rotary inertia of car differential
η = Transmission efficiency
n_o = Differential gear ratio
r_w = tire radius [m]

$$\pm : \begin{cases} (+)\text{with the car in acceleration (ascending)} \\ (-)\text{With the car in deceleration (descending)} \end{cases}$$

5) The Total Resistive Force

The total resistance = Drag Force + Rolling resistance + Gradient resistance+ Inertia Resistance

Hence,
The total resistance $= \frac{1}{2}\,C_D\,A\,\rho\,u^2$ + G. f. cos θ_r ± G sin θ_r ± (m+ m$_{eq}$). a

Resistive Torque= $T_v = r_w$. Resistive Force

$$T_v = r_w * (\ \tfrac{1}{2}\,C_D\,A\,\rho\,u^2\ + \text{G. f. cos }\theta_r\ \pm \text{ G sin }\theta_r \pm (m + m_{eq}).\,a) \tag{66}$$

In dimensionless form:

$$T_v{}^{\bullet} = (A_1)\,[f.cos\theta_r + sin\,\theta_r] + (A_2)\,U^{\bullet 2} + (A_3)\,U^{\bullet} \tag{67}$$

Where:

$A_1 = \dfrac{r_w \cdot G}{\sigma\, \Omega\, c^3}$, $A_2 = \dfrac{1}{2}\, C_D\, A\, \rho\, \dfrac{\Omega^2\, r_w^2}{G}$, $A_3 = \dfrac{m\, \Omega\, r_w}{G}$ $+$

$\dfrac{J_r\, \Omega}{G\, r_w} + \dfrac{J_w \cdot n_o^2 \cdot n^2 \cdot \eta\, \Omega}{G\, r_w}$

From Fig.3 we can obtain the dynamic equation of the vehicle angular speed as follows:

$$J_r\, \dot{\omega}_v + B_r\, \omega_v = T_o n_o - T_v \qquad (68)$$

E. Evaluation of the load torque on CVT T_o^*

T_o^* can be obtained from the following relation :

$$T_o^* = T_v^* \cdot \dfrac{\omega_v^*}{\omega_s^*}$$

III. NUMERICAL SOLUTION, RESULTS AND DISCUSSION

From (1), (5), (36), (40) and (68), the governing ordinary differential equations of the vehicle mathematical model can be written as follows:

$$\dfrac{d\omega_e^*}{dt^*} = (T_e^* - T_{cl}^*) - \left(\dfrac{B_e}{J_e\, \Omega}\right)\omega_e^*$$

$$\dfrac{d\omega_{cl}^*}{dt^*} = (T_{cl}^* - T_p^*) - \left(\dfrac{B_{cl}}{J_{cl}\, \Omega}\right)\omega_{cl}^*$$

$$\dfrac{d\omega_s^*}{dt^*} = (T_s^* - T_o^*) - \left(\dfrac{B_s}{J_s\, \Omega}\right)\omega_s^*$$

$$\dfrac{d\omega_p^*}{dt^*} = \dfrac{1}{1-s}\left[\dfrac{(T_s^* - T_o^*)}{n} - \right.$$
$$\left(\dfrac{B_s}{J_s\, \Omega}\right)\omega_s^* - \left(\dfrac{1}{n^2}\dfrac{dn}{dt^*}\right)\omega_s^* + \omega_p^* \cdot \dfrac{ds}{dt^*} \left.\right]$$

$$\dfrac{d\omega_v^*}{dt^*} = (T_o^*\, n_o - T_v^*) - \left(\dfrac{B_r}{J_r\, \Omega}\right)\omega_v^*$$

In which, J_e, is the rotary inertia of engine; J_{cl}, is the rotary inertia of clutch; J_s is the rotary inertia of the secondary pulley of CVT; J_r is the rotary inertia of the car differential; and J_w is the rotary inertia of the wheels. And B_e, B_{cl}, B_s and B_r represent the equivalent damping coefficient of each axis respectively

A. The initial Conditions

At the beginning of the motion when t*=0, the initial conditions are:

$$T_p^* = T_{cl}^* = T_e^*$$
$$\omega_e^* = \omega_{cl}^* = \omega_p^* = 1$$
$$\omega_s^* = \omega_p^* \cdot n$$
$$\omega_v^* = \dfrac{\omega_s^*}{n_o}$$

B. Numerical Solution

The ordinary differential equations were numerically solved using ode23 MATLAB solver. The ode23 solver uses second and third order Runge-Kutta-Fehlberg integration with variable step size. The angular speeds of each component of the model were integrated with time. The results are plotted in Fig.13
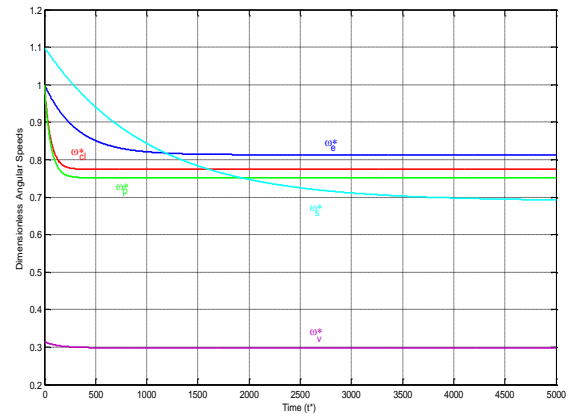
From Fig.13, the following results are obtained:

a) The dimensionless angular speed of engine ω_e^* , initially starts at $\omega_e^* = 1$ (equivalent to an angular speed of 210 rad/s). It then decreases until it becomes steady at a dimensionless angular speed of 0.82, after a time of approximately 5 seconds (equivalent to a non-dimensional time $t^* = 1050$).

b) The dimensionless angular speed of clutch ω_{cl}^* , starts at $\omega_{cl}^* = 1$. It then decreases until it becomes steady at a dimensionless angular speed of 0.78, after a time of approximately 1 second.

c) The dimensionless angular speed of CVT primary pulley ω_p^* , starts at $\omega_p^* = 1$. It then decreases until it becomes steady at a dimensionless angular speed of about 0.75, after an actual time of approximately 1 second.

d) The dimensionless angular speed of CVT secondary pulley ω_s^* , starts at $\omega_s^* = n = 1.1$. It then decreases until it becomes steady at a dimensionless angular speed of about 0.7, after a time of approximately 14 seconds.

e) The dimensionless angular speed of vehicle ω_v^* , starts at $\omega_v^* = \dfrac{n}{n_o} = \dfrac{1.1}{3.5} = 0.3143$. It then decreases until it becomes steady at a dimensionless angular speed of about 0.3, after a time of approximately 0.7 seconds.

IV. CONCLUSIONS

In this paper, a mathematical model for a complete vehicle equipped with CVT is constructed. The model simulates the whole vehicle dynamics. A separate model for every component of the vehicle; the engine, clutch, CVT, car differentials, wheels and car body, was constructed.
The slip between the belt and the pulley along with the CVT traction curve were taken into consideration in the mathematical model. The kinematic and geometric equations were formulated for the whole system.

The differential equations for the angular velocities for every component in the system were formulated. These equations were numerically solved in order to predict the behavior of the system. Plotting the angular speeds with time, the numerically simulated results show that the system becomes steady after a short period of time. The graphical representation of the system's dynamical response demonstrates that the simulation model established represent the system efficiently.

REFERENCES

[1] G. Gerbert, Force and slip behavior in V-belt drives, Acta Polytechnica Scandinavica, Mechanical Engineering Series, No. 67, Lund Technical University, Lund, Sweden, 1972.

[2] G. Gerbert, Metal V-belt mechanics, in: ASME Design Automation Conference, Advances in Design Automation, ASME Paper No. 84-DET-227, Boston, MA, 1984, 9p.

[3] G. Gerbert, Belt slip – a unified approach, ASME Journal of Mechanical Design 118 (3) (1996) 432–438.

[4] H. Kim, J. Lee, Analysis of belt behavior and slip characteristics for a metal V-belt CVT, Mechanism and Machine Theory 29 (6) (1994) 865–876.

[5] H. Lee, H. Kim, Analysis of primary and secondary thrust for a metal CVT, Part 1: new formula for speed ratio–torque–thrust relationship considering band tension and block compression, in: Transmission and Driveline Symposium, SAE Paper No. 2000-01-0841, SAE special publication (SP-1522), 2000, pp. 117–125.

[6] B. Bonsen, T.W.G.L. Klaassen, K.G.O. van de Meerakker, M. Steinbuch, P.A. Veenhui36zen, Analysis of slip in a continuously variable transmission, in: Proceedings of IMECE'03, 2003 ASME International Mechanical Engineering Congress, Paper No. IMECE2003-41360, Washington, DC, USA, vol. 72, No. 2, November 15–21, 2003, pp. 995–1000.

[7] D. Sferra, E. Pennestri, P.P. Valentini, F. Baldascini, Dynamic simulation of a metal-belt CVT under transient conditions, in: Proceedings of the ASME 2002 Design Engineering Technical Conference, Paper No. DETC02/MECH-34228, Montreal, Canada, vol. 5A, September 29–October 2, 2002, pp. 261– 268.

[8] M. Bullinger, F. Pfeiffer, Elastic modelling of bodies and contacts in continuous variable transmissions, Multibody System Dynamics 13 (2) (2005) 175–194.

[9] M. Bullinger, F. Pfeiffer, An elastic model of a metal V-belt CVT, Proceedings in Applied Mathematics and Mechanics (PAMM) 2 (2003) 112 113.

[10] H. Sattler, Efficiency of metal chain and V-belt CVT, in: Proceedings of the International Congress on Continuously Variable Power Transmission CVT'99, Eindhoven, The Netherlands, September 16–17, 1999, pp. 99–104.

[11] G. Carbone, L. Mangialardi, G. Mantriota, The influence of pulley deformations on the shifting mechanism of metal belt CVT, ASME Journal of Mechanical Design 127 (1) (2005) 103–113.

[12] G. Carbone, L. Mangialardi, B. Bonsen, C. Tursi, P.A. Veenhuizen, CVT dynamics: theory and experiments, Mechanism and Machine Theory 42 (4) (2007) 409–428.

[13] A.F.A. Serrarens, M. Dassen, and M. Steinbuch. Simulation and control of an automotive dry clutch. In Proceedings of the American Control Conference, pages 4078–4083, Boston, USA, 2004.

[14] A. F. A. Serrarens. Coordinated Control of The Zero Inertia Powertrain. PhD thesis, Technische Universiteit Eindhoven, 2001.

[15] G. Gerbert, F. Sorge, Full sliding adhesive-like contact of V-belts, ASME Journal of Mechanical Design 124 (4) (2002) 706–712.

[16] B. Bonsen, R.J. Pulles, S.W.H. Simons, M. Steinbuch, P.A. Veenhuizen, Implementation of a slip controlled CVT in a production vehicle, in: Proceedings of the 2005 IEEE Conference on Control Applications, Toronto, Canada, August 28–31, 2005, pp. 1212–1217.